FROM MERIS TO OLCI AND SENTINEL 2: HARMFUL ALGAL BLOOM APPLICATIONS & MODELLING IN SOUTH AFRICA

L. Robertson Lain[(1)], S. Bernard[(2)], H. Evers-King [(1)], M. W. Matthews[(1)], M. Smith [(1)]

[(1)]*Oceanography Department, University of Cape Town, Private Bag, Rondebosch 7700, South Africa.*
Email:lislrobertson@gmail.com
[(2)]*CSIR, 15 Lower Hope St, Rosebank 7700, South Africa*
Email:sbernard@csir.co.za

ABSTRACT

The Sentinel 2 and 3 missions offer new capabilities for Harmful Algal Bloom (HAB) observations in Southern Africa and further afield on the African continent where there is a great need for improved monitoring of water quality: both in freshwater resources where eutrophication is common, and in vulnerable coastal ecosystems. Two well validated algorithms - Equivalent Algal Populations (EAP) & Maximum Peak Height (MPH) - available for operational use on eutrophic waters are described. Spectral remote sensing reflectances (R_{rs}) and inherent optical properties (IOPs) are characterised via measurement and modelling of phytoplankton assemblages typical of high biomass algal blooms of the Southern Benguela and inland waters of South Africa. Sensitivity to phytoplankton functional types (PFTs) is investigated, with focus on optically significant biological characteristics e.g. particle size distribution and intracellular structure (including vacuoles).

1. INTRODUCTION

There is a pressing need in both coastal and inland resource management systems for routine HAB detection and water quality indicators. Eutrophication and harmful cyanobacterial blooms are widespread in South African inland water bodies. Since South Africe suffers from water scarcity, surface reservoirs constitute the country's primary water resources for potable uses, industry, agriculture and recreation. The St Helena Bay area of the Southern Benguela upwelling system has a well established history of Harmful Algal Blooms (HABs), affecting commercial, subsistence and recreational fisheries activities, and which regularly threaten ecosystem health due to the proliferation of toxic species and/or subsurface anoxia leading to massive faunal mortalities.

2. CHARACTERISING HIGH BIOMASS R_{rs}

A 10 year archive of i*n situ* bio-optical measurements has been compiled from the S. Benguela, mostly during the bloom season (late summer). Three main phytoplankton groups are found to be optically distinct and the main contributors of response to the light field in Benguela bloom conditions: diatoms & dinoflagellates, nanophytes (including chlorophytes) and cryptophytes (representing, in the Benguela, the autotrophic ciliate *Mesodinium rubrum*). The inland waters sampled are typically dominated by cyanobacteria, with some dinoflagellate species present.

Tethered Satlantic Radiometer Buoy (TSRB) measurements from the Benguela, processed to R_{rs} using the Satlantic proprietary software PROSOFT, are presented in 3 Chl-a classes in Fig. 1 (a).
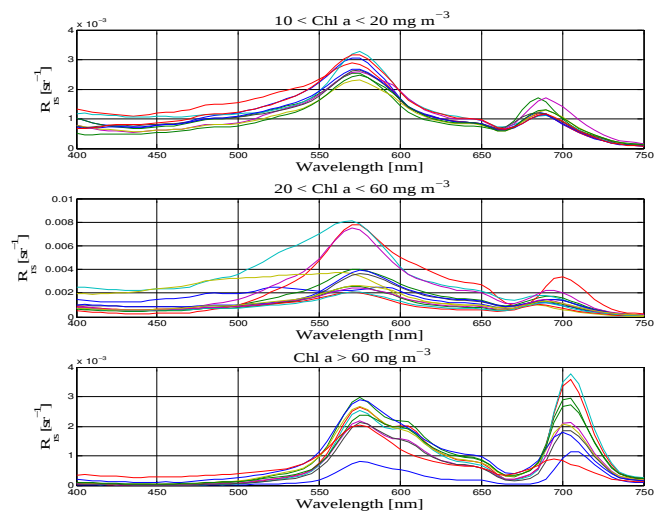

Figure 1 (a). Measured R_{rs} (S. Benguela)

The blooms represented here are mostly diatom dominated up to Chl-a of 20 mg/m³, occasionally *M. rubrum* dominates with an identifiable widened peak at 510 nm displaying the additional absorption characteristics of the pigment phycoerythrin. The signal dampening effect of cell size can be seen in the magnitude of the R_{rs} for certain samples, e.g. the blue line at the very bottom of the Chl-a>60 mg/m³ category represents an *Alexandrium catenella* bloom with a Chl-a of 309 mg/m³. *A. Catenella* is a large dinoflagellate of around 30 μm diameter, and characteristically forms chains which may have a further signal dampening effect. The majority of samples are dinoflagellate-

dominated at very high (>60 mg/m³) biomass. At lower biomass, the signal in the red is primarily fluorescence with quantum yields of <0.5% [1, 2]. Some shift towards 709 nm is seen as absorption/ backscattering processes become important in combination with fluorescence. At high biomass, an inflection point appears at 620 nm, related to secondary Chl-a and Chl-c absorption peaks.
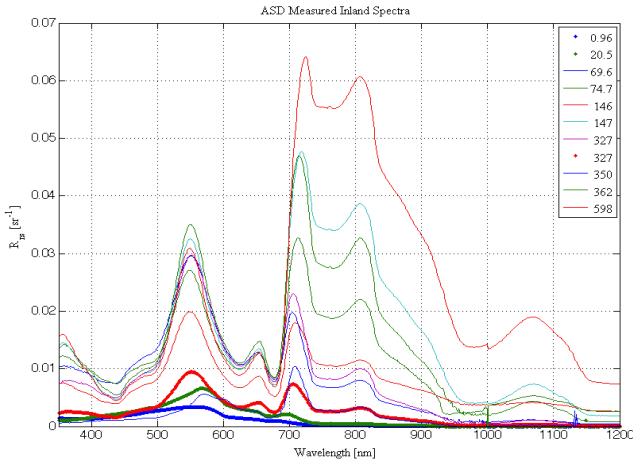

Figure 1 (b). Measured R_{rs} (inland waters) Chl-a concentrations are inset.

Many of the same spectral features can be observed in the ASD-measured R_{rs} from the inland water bodies. It should be noted though that where the Benguela waters can be typified as high biomass Case 1, the inland samples are generally representative of waters with a total suspended solids (TSS) count of 0.1 to 300 mg/l. They are dominated either by *Microcystis* cyanobacteria or dinoflagellate *Ceratium* assemblages. Phytoplankton typically contributes 20% to 100% of the R_{rs} signal [3]. The R_{rs} for eukaryotic assemblages (thicker lines, dot in legend) are very similar to those measured in the Benguela. However R_{rs} representing vaculoate prokaryotic (cyanobacteria) populations are much brighter due to the effect of the air-filled vesicle on the cells' refractive index [4]. The peak near 660 nm caused by phycocyanin and Chl-a pigment absorption bands at 620 and 665 nm is an identifiable feature of *Microcystis*-dominated assemblages. The absorption minima of water at 750 and 990 nm also become important spectral features.

3. COUPLED RADIATIVE TRANSFER, ALGAL POPULATION MODELLING

A solid modelling capability is critical to the understanding of phytoplankton-driven bio-optical variability, and PFT analysis. A comprehensive IOP model is also a central component of any inversion scheme.

The Equivalent Algal Populations (EAP) model (Robertson *et al.* in prep) is coupled with Ecolight radiative transfer software (Sequoia Inc.) to model phytoplankton IOPs and R_{rs}. The EAP model is based on a 2 layered sphere geometry [5] and is well validated for these high biomass conditions.

Modelling from first principles (cell refractive indices mathematically derived from measured phytoplankton-specific absorption, and the size distribution) allows explicit calculation of component IOPs and theoretical optical quantities that form the basis of a coherent understanding of their relationship to each other and resulting water-leaving signal e.g. shape factors used in the reflectance approximation, such as the f/Q factor. The model allows admixtures of various phytoplankton types, population size distributions (e.g. standard normal, inverse gaussian, jungian) with varying statistical parameters e.g. effective variance. Other variables include the chlorophyll-a density per cell, and phase function selection (constant b_b/b vs spectrally variable b_b/b, for example). Studies are under way to determine the sensitivity of the model to small changes in these quantities. While the 2-layered spheres are phytoplankton-specific, additional components may be added to simulate naturally occurring water types. Non-phytoplankton contributions can be modelled in various ways, and currently a default scheme is used whereby a combined gelbstoff and non-algal absorption term varies non-linearly with increasing Chl-a, and a simple spectral slope non-algal backscattering term is used [6]. The fluorescence quantum yield varies from 0.8% to 0.1% as eutrophication increases [2].

The EAP model emphasises and depends heavily on the size-related aspects of assemblage modelling due to the structure of the 2 layered sphere as the IOP determinant. As Chl-a concentration increases from 0.1 to 300 mg/m³ (in Fig. 2 (a) IOPs are shown for idealised diatom/ dinoflagellate assemblage, effective diameter of 16 µm), spectral detail in the total scatter becomes significant. This has an impact on the total backscattering profiles, where it can be seen that variability in the spectral shape becomes substantial at even relatively low Chl-a concentrations (around 3 mg/m³). The ability to detect distinct phytoplankton classes depends largely on this detailed spectral backscattering (see Fig. 3).

Comparing equivalent Chl-a concentrations within the same modelled population types, it can be seen that at a concentration of 1 mg/m³ there is little to distinguish spectrally between a diatom/dinoflagellate-dominated sample and a cryptophyte-dominated sample. However at 10 mg/m³ this ability increases due to the separation of the maximum phytoplankton Chl-a absorption peak at 560 nm into its distinctive phycoerythrin peak in the cryptophyte sample. By 100 mg/m³ the spectra are significantly different spectrally.
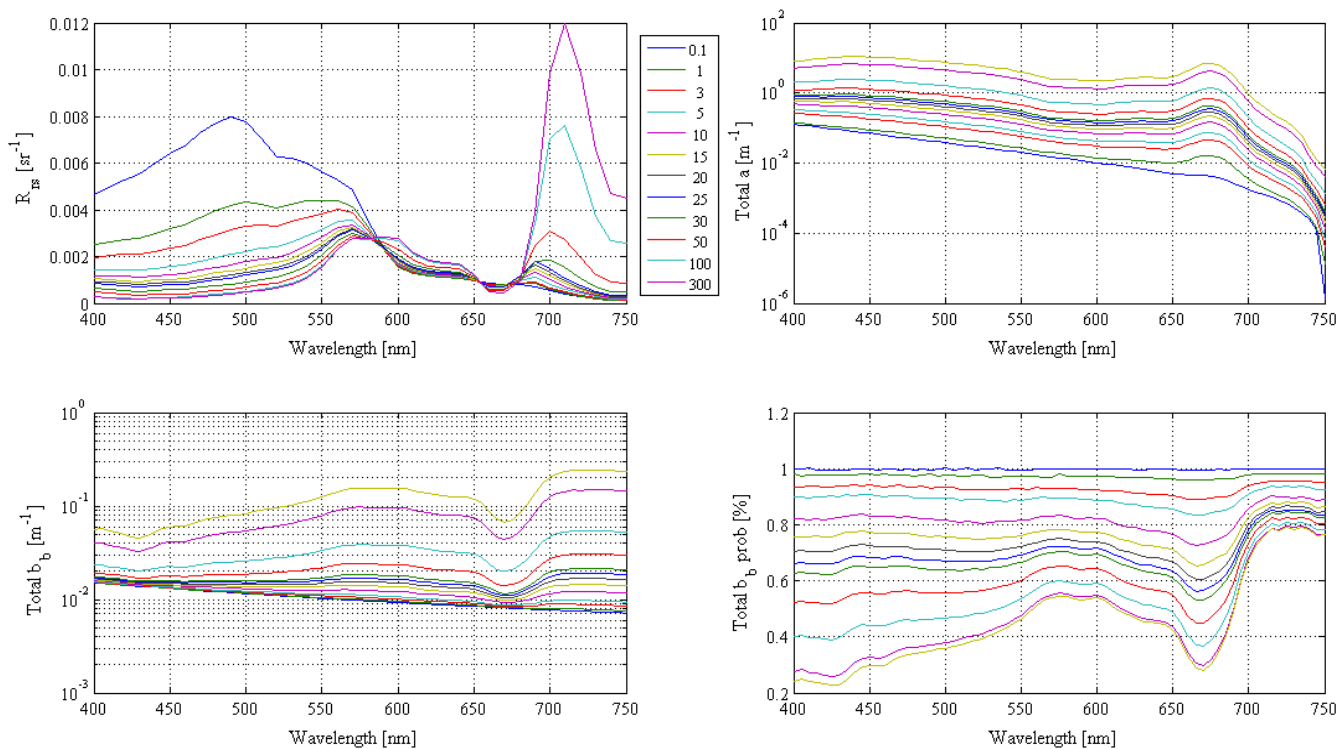
Figure 2 (a). Modelled R_{rs} and IOPs for an idealised diatom/dinoflagellate assemblage, with effective diameter 16 µm and non-phytoplankton components as described in text.
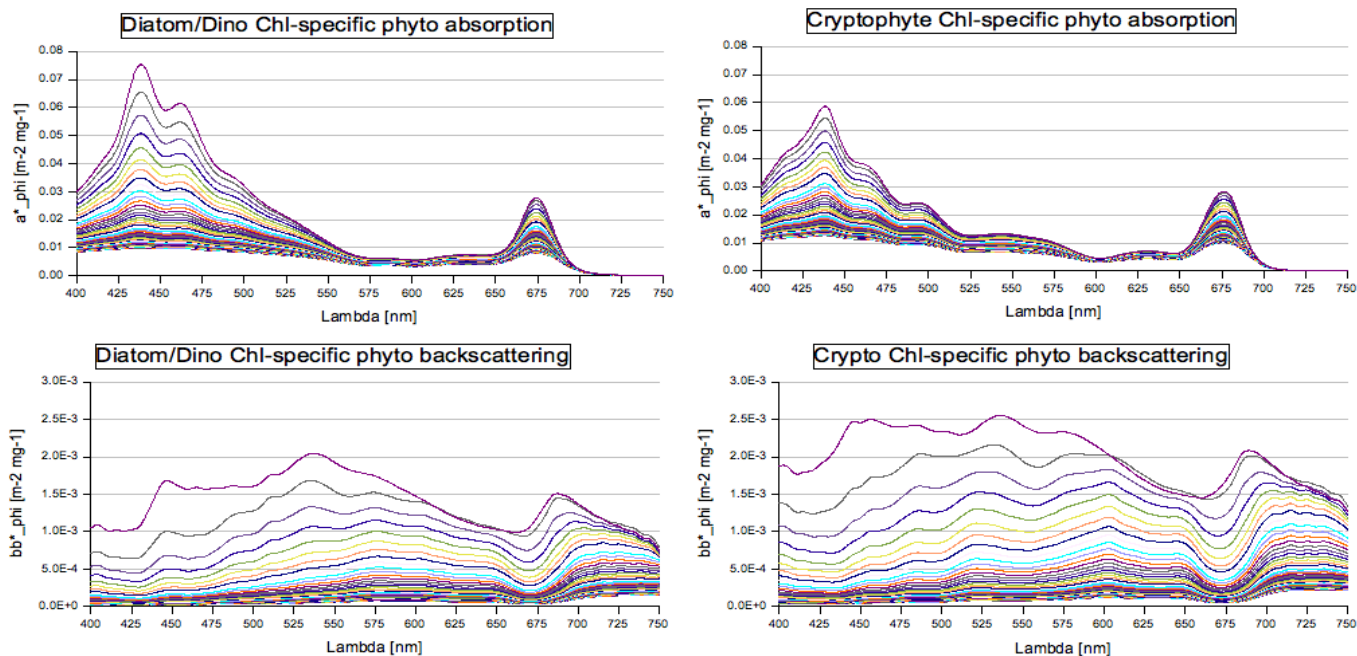

Figure 2 (b). Modelled Chl-a-specific absorption and backscattering for two different assemblage types: diatom/dinoflagellate- and cryptophyte-dominated
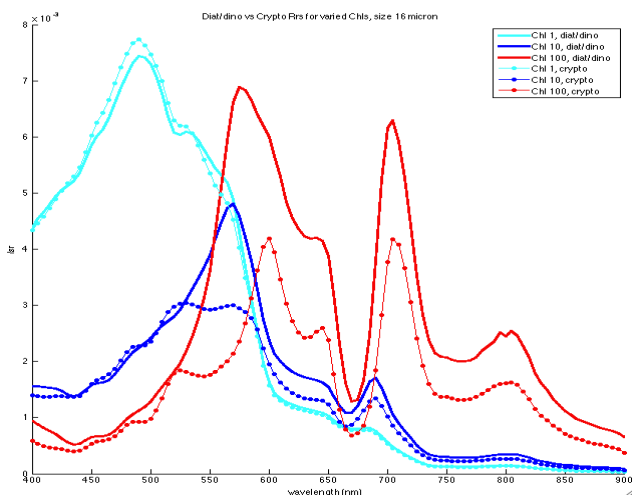
Figure 3. Modelled R_{rs} at selected Chl-a concentrations for two different phytoplankton types: diatom/dinoflagellate- and cryptophyte-dominated

Synthetic data can be generated in this way for any defined ranges of biophysical parameters, in imitation of the variability in naturally occurring populations and aquatic conditions. Ongoing work is focused on systematically constraining the dataset to ensure that natural variability is adequately represented, based upon established abundance and allometric evidence [7]. Constrained as such, this dataset can be used for algorithm development and testing. Exploratory efforts towards the development of a water type classification scheme look promising as a framework for further describing the variability of IOP subcomponents.

4. EAP INVERSION

The coupled EAP-Ecolight model is also well validated as an inversion model (Fig.s 4(a) & 4(b), Evers-King in prep). The inversion can be performed on *in situ* hyperspectral water-leaving reflectance or on atmospherically corrected L2 satellite water-leaving radiance data. The algorithm was used extensively for the retrieval of Chl-a concentration and changes in population effective diameter from L2 MERIS images as a component of the routine monitoring and HAB detection activities in the Southern Benguela from 2002 until the demise of Envisat in 2012 [8,9].

Fig. 4 (b) shows the errors on the retrieval of effective diameter and Chl-a: the model performs best (errors of less than 30%) at larger effective diameters where chlorophyll concentrations are above 10 mg/m^3 - i.e. in bloom conditions. Where Chl-a concentrations fall below 10 mg/m^3 it appears there is not sufficient size-related R_{rs} signal to retrieve effective diameter directly, within suitable confidence intervals.
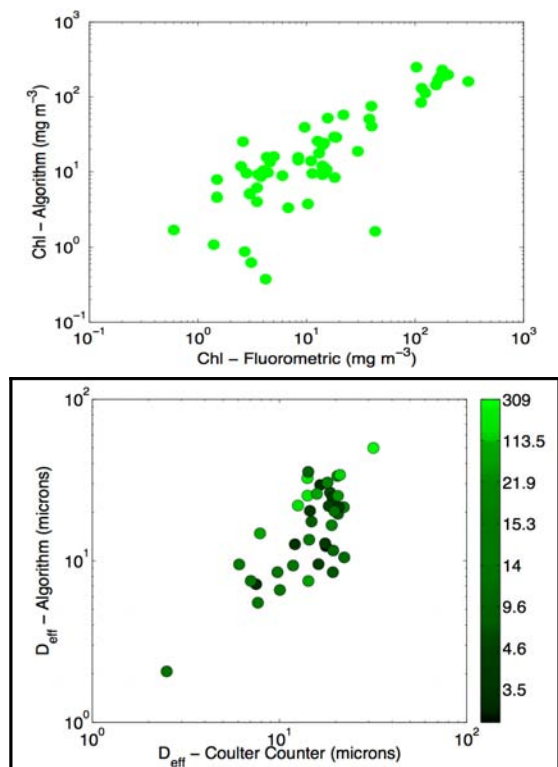

Figure 4 (a). EAP inversion validation for Chl-a retrieval (top) and effective diameter (bottom). R^2 for Chl-a is 0.89 with $p<0.005$, R^2 for size is 0.5 with $p<0.005$.
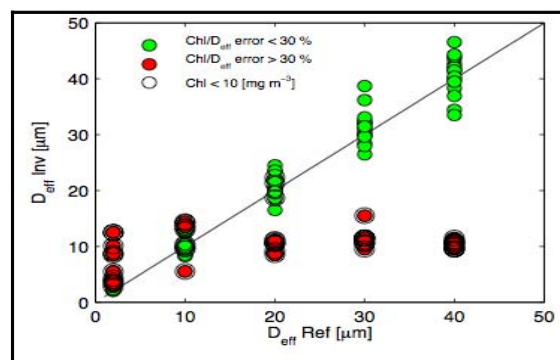

Figure 4 (b). EAP inversion validation: errors on retrieval of chlorophyll and effective diameter

5. MPH ALGORITHM

The Maximum Peak Height (MPH) algorithm [3] detects trophic status (chlorophyll-a), cyanobacterial blooms and the presence of surface scums and floating vegetation. The algorithm uses a baseline subtraction procedure to calculate the height of the dominant peak across the red and near-infrared MERIS bands between 664 and 885 nm caused by sun-induced chlorophyll fluorescence (SICF) and particulate backscatter. One

great advantage of this approach is that where the available spectral bands are in close proximity, the differential spectral signal is sufficiently large that the algorithm can be used on TOA (top of atmosphere) data corrected only for gaseous absorption and Rayleigh scattering, and so avoids the problems associated with the correction of aerosol absorption over small inland water bodies. The algorithm is specifically designed for MERIS wavebands from TOA, and is therefore ideal for use with OLCI. It may be possible to employ some analogous scheme on Sentinel 2 data but with some loss of sensitivity in lower biomass conditions as there is no explicit fluorescence band on Sentinel 2.
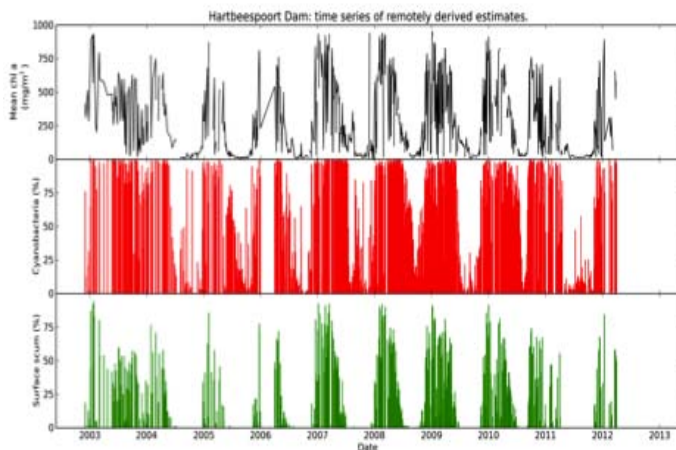

Figure 5. 10 year time series of phytoplankton biomass (top), percentage cyanobacteria (middle), and percentage surface scums (bottom) for Hartbeespoort Dam, using the MPH algorithm applied to MERIS FR data. (Matthews, in prep)

6. SATELLITE PRODUCTS

South African HAB observations depended heavily on MERIS both operationally and for research, due to the highly optimised nature of the sensor for eutrophic waters. Significant progress was also made with MERIS in terms of processing, storage and dissemination capabilities. These systems can now be adapted in readiness for OLCI. There is a strong dependence on a closely clustered set of bands in the red-NIR range, most importantly the 709 band, for HAB detection and monitoring at high biomass. Sentinel 2, with much increased spatial resolution and good signal-to-noise ratio, offers sufficiently good spectral resolution in this range to be of considerable value for inland HAB and water quality applications.

OLCI, with its bands optimised for the retrieval of reflectances over dark surfaces, presents many further opportunities for algorithm development and application.
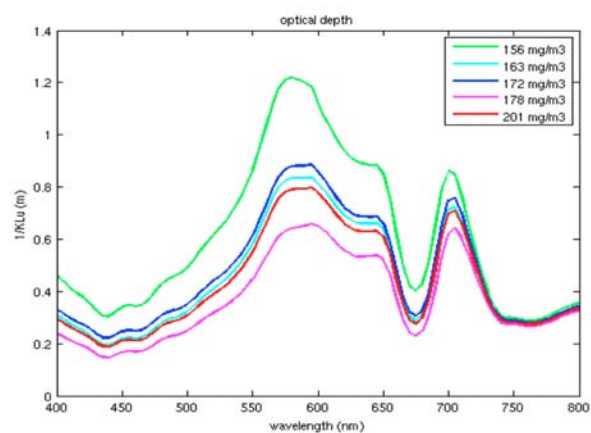
7. CHALLENGES

Spatial and temporal variability of blooms is significant when matching *in situ* to satellite data and has to be addressed with extensive documentation of each sampling/measurement activity. Aside from logistical difficulties, in eutrophic and hypertrophic water bodies, measurements are frequently made at depths approaching one optical depth. Instrument performance and reliability may be uncertain under these conditions. For example, the TSRB measures upwelling irradiance L_u at 0.66 m. Fig. 6 shows the optical depths ($1/K_{Lu}$) for various high biomass samples from the Benguela (inversely modelled from the measured R_{rs} using EAP IOPs).

Figure 6. Optical depth of selected high biomass samples

The calculation of the diffuse upwelling radiance coefficient (K_{Lu}) remains a challenge. This quantity is necessary for the extrapolation of $L_u(z)$ as measured by an in-water radiometer, through the surface to R_{rs}. Literature K_{Lu}s available for Case 1 waters such as those of Albert and Mobley [10] are typically lower than those modelled by Ecolight using the EAP inversion technique. The selection of K_{Lu} for the processing of measured radiometric data obviously has a significant impact on the resulting R_{rs}.

Other measurement challenges include AC-type absorption measurements, for e.g., those measured at Chl-a concentrations of over 500 mg/m^3 were an order of magnitude lower than those derived from filter pad measurements because the samples were too viscous to move through the detector properly.

There remains a need for the development of measurement protocols for eutrophic water conditions, similar in breadth and quality to those prepared for SeaWiFS validation by Mueller *et al.* [11].
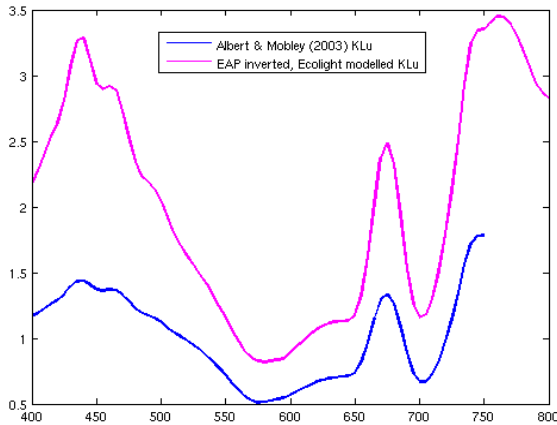
Figure 7. Albert and Mobley (2003) K_{Lu} vs. EAP inverted, Ecolight modelled K_{Lu} for a sample with measured Chl-a of 309 mg/m^3.

8. REFERENCES

1. Dierssen H.M., R.M. Kudela, J.P. Ryan, R.C. Zimmerman (2006) Red and black tides: Quantitative analysis of water-leaving radiance and perceived color for phytoplankton, colored dissolved organic matter, and suspended sediments *Limnol. Oceanogr*., 51(6), 2006, 2646–2659

2. Ostrowska, M., B. Woźniak, J. Dera (2012) Modelled quantum yields and energy efficiency of fluorescence, photosynthesis and heat production by phytoplankton in the World Ocean. *OCEANOLOGIA*, 54 (4), 2012. pp. 565 – 610.

3. Matthews, M. W., S. Bernard, & L. Robertson (2012). An algorithm for detecting trophic status chlorophyll-a, cyanobacterial-dominance, surface scums and floating vegetation in inland and coastal waters. *Remote Sensing of Environment*, *124*, 637-652.

4. Matthews, M. W., & Bernard, S. (2013). Using a two-layered sphere model to investigate the impact of gas vacuoles on the inherent optical properties of M. aeruginosa. *Biogeosciences Discussions*, *10*(6), 10531-10579.

5. Bernard, S., T.A. Probyn, and A. Quirantes (2009) Phytoplankton optical models with two layered spheres. *Biogeosciences Discuss*., 6, 1497–1563, 2009

6. Roesler, C.S., and M.J. Perry. (1995). In situ phytoplankton absorption, fluorescence emission, and particulate backscattering spectra determined from reflectance. *J. Geophys. Res*., C100: 13 279-13 294.

7. Irwin, A. J., Z.V. Finkel, O.M. Schofield, & P.G. Falkowski (2006). Scaling-up from nutrient physiology to the size-structure of phytoplankton communities. *Journal of Plankton Research*, *28*(5), 459-471.

8. Fawcett, A., G.C. Pitcher, S. Bernard, A. Cembella, & R.M. Kudela (2007). Contrasting wind patterns and toxigenic phytoplankton in the southern Benguela upwelling system. *Marine Ecology Progress series 348*, 19-31.

9. Bernard S., R. Kudela, P. Franks, W. Fennel, A. Kemp, A. Fawcett, G. Pitcher. (2006). The requirements for forecasting harmful algal blooms in the Benguela. In: V. Shannon, G. Hempel, P. Malanotte-Rizzoli, C. Moloney, J. Woods (eds) *Benguela: predicting a large marine ecosystem*. Elsevier, Amsterdam, p 273–294

10. Albert, A., & C. D. Mobley (2003). An analytical model for subsurface irradiance and remote sensing reflectance in deep and shallow case-2 waters. *Opt. Express*, *11*(22), 2873-2890.

11. Mueller, J. L., G.S. Fargion, C.R. McClain, S. W. Brown, D.K. Clark, ... & R.A Barnes (2003). Ocean Optics Protocols For Satellite Ocean Color Sensor Validation, Revision 5, Volume VI: Special Topics in Ocean Optics Protocols, Part 2. *NASA Tech. Memo*, *211621*.